

Reduced-order Modeling of Parameter Variations for Parameter Identification in Rubber Curing

Tobias Frank^a, Mark Wielitzka, Matthias Dagen and Tobias Ortmaier

Institute of Mechatronic Systems, Leibniz University Hanover, An der Universitaet 1, Garbsen, Germany

Keywords: Large-scale Systems, Parameter Identification, Model Order Reduction, Linear Parameter-variant Systems.

Abstract: A reduced-order modeling approach for thermal systems with varying parameters in rubber curing processes is presented in this manuscript. For complex geometries with multiple components a finite element analysis with fine mesh elements is often the only feasible approach to calculate temperature distributions over time. A major drawback, however, is the resulting large system scale, which entails high computation times. Thus, real-time capable execution or a high number of iterations to solve for optimization problems are infeasible approaches. Model order reduction algorithms are a promising remedy, but physically interpretable parameter preservation is not obtained, when using common approaches. Thus, a method to extract parameter dependencies from numerical element matrices and reduce the model order is presented in this manuscript. Preservation of physically interpretable parameters is accomplished by applying linear reduction projectors to affine interpolated system matrices. Thus, parameter variations can be accounted for without costly recalculation of reduction projectors. Hence, a computation efficient model description is obtained, enabling a tunable balancing between computation time and accuracy. To demonstrate the effectiveness of the approach, parameter identification of material properties and heat transition coefficients is performed and validated with measurement data of two different sample systems. For the largest sample system computation time has been reduced from half an hour for a full order simulation to an averaged time of 0.3 s, with approximation error of 0.7 K.

1 INTRODUCTION

Manifold model-based process planning and control methods require accurate thermal modeling to obtain satisfying results. A good example is industrial curing of rubber compounds or polymer composites, where reliable process sequences are decisive for high product quality. One curing sequence consist of a heating and subsequent cooling phase. Uncured compounds are placed into a preheated mold to get final product shape and start temperature-dependent chemical reactions for polymer chain cross-linking. The product can contain multiple compounds with different material properties and the curing process is planned so that every compound reaches a desired cross-linking (cure) status at certain points of interest or throughout its whole cross-section. Experiments can be conducted to empirically determine mold temperatures and heating duration, however they tend to be very time consuming. Thermal modeling and cure status extrapolation can be used to optimize the process offline prior to vulcanization start (Aleksendrić et al.,

2016). Furthermore, different process aspects such as energy consumption and product quality can be optimized by iteratively solving a minimization problem (Bosselmann et al., 2018). In order to build a suitable process model, product geometry and material properties are often set in a finite element analysis to solve for temperature distributions over time and calculate the overall cure status, when vulcanization reactions have finished. However, accurate thermal modeling can be impeded by varying material properties or geometric parameters. Since rubber is a natural product, thermal conductivity, density and specific heat can vary significantly from one batch to another. Similarly, tolerances and deviations in the processes prior to curing, can cause compound or geometrical variations, that can further affect offline process planning. Ultimate goal is a parameter-dependent system description, that can be quickly adapted for a specific product with measured parameters prior to the curing process. Process parameters such as mold temperatures and heating duration can then be quickly adapted, using a cost function and gradient-based optimization. Subsequent to a pre-

^a  <https://orcid.org/0000-0001-9289-4467>

cise process planning, determined process parameters have to be maintained online. Industrial heating systems such as molds need to be controlled properly to ensure a desired temperature distribution at contact surfaces or product interfaces (Wang et al., 2015). Model-based control approaches are favourable, since multiple process criteria and limitations can be accounted for. However, unknown or temperature dependent boundary conditions to the ambient can lead to disturbances or model errors. Furthermore, it is beneficial to identify mold material properties, thermal resistances and heat transitions, due to material contact surfaces or components with unknown assembly. Thus, a computation-efficient and parameter-dependent system description is required, to enable real-time computation for model-based control and state estimation or to perform high amounts of iterations in short time to solve for optimization problems.

Besides curing processes, multiple approaches have been introduced to incorporate thermal models in process control approaches. If applicable, model simplifications, such as reduction of spatial dimension, using symmetry or neglecting complex geometric structures, are an easy and well used remedy. Speicher et al. (Speicher et al., 2014) used a lower spatial dimension model to reduce computation complexity and estimate plate temperatures in a hot rolling process. Furthermore, linearizations are applicable, if the system maintains in a specific operating area. In this case linear model order reduction can be a powerful tool to lower system scale (Yuan et al., 2017), (Benner et al., 2019). If these simplifications are improper, parametric model order reduction methods to approximate large scale systems can be used, but yield possible limitations in number of accountable parameters, online adaption and reduced system order (Benner et al., 2015). A proper choice to reduce the model would be Proper Orthogonal Decomposition (POD) (Astrid, 2004). This approach for nonlinear systems is especially effective with the use of discrete empirical interpolation (DEIM) (Chaturantabut and Sorensen, 2010). However, sample trajectories (snapshots) of already validated full order models or a high amount of measurement data are required, when a vast amount of varying parameters occur. Sun et al. used balancing and POD to model parameter uncertainties by lumping parameters into the input vector and incorporate them into the reduction process (Sun and Hahn, 2006).

In this work a novel method for thermal modeling with accountable parameter variations is proposed. The system description can be directly derived from finite element analysis. Main achievements are formulation of thermal linear parameter-variant (LPV)

systems from nonlinear partial differential equations, model order reduction of LPV systems, and parameter preservation to enable optimization and identification procedures. Furthermore, state-dependent parameter changes as caused temperature-dependent boundary conditions can be accounted for during simulation, enabling a balancing between computation time and accuracy.

2 METHODS

In this section a thermal modeling approach is described in order to achieve a linear parameter-dependent system description from numerical element matrices of a FEA. Subsequently, model order reduction of the LPV system and parameter preservation is explained. Ultimately, a computation efficient system description with approximated temperature dependent boundary conditions is gained and used for results in Section 3.

2.1 Thermal Modeling

The spatial-temporal dependent temperature distribution $T(z, t)$ of a distributed parameter system within domain $\Omega \subset \mathbb{R}^{n_{\text{dim}}}$, $\forall z = (z_1, \dots, z_{n_{\text{dim}}})^T \in \Omega$ at time $t \in \mathbb{R}^+$ and dimension $n_{\text{dim}} \in \{1, 2, 3\}$ can be described as a scalar field with parabolic partial differential heat equations (PDEs) and *Fourier's* law, leading to infinite dimensional equation:

$$c(z)\rho(z)\frac{\partial T(z, t)}{\partial t} = \text{div}(\Lambda(z)\nabla T(z, t)) + \omega(z, t). \quad (1)$$

The ∇ -operator denotes partial derivatives with respect to z . Internal heat sources are expressed as ω in $[\text{Wm}^{-3}]$. Material properties c and ρ are specific heat and density. Λ denotes the thermal conductivity tensor which can account for anisotropic heat conduction. The following three assumptions are made for the material coefficients:

Assumption 1. All material properties $c(z)$, $\rho(z)$, and $\Lambda(z)$ are time and state invariant.

Assumption 2. System domain Ω consists of multiple components Ω_j , $\Omega = \bigcup_{j \in \{1, \dots, n_{\text{comp}}\}} \Omega_j$, $j \in \{1, \dots, n_{\text{comp}}\}$, $n_{\text{comp}} \in \mathbb{N}^+$ made of homogeneously distributed materials with properties $c(z_j) \cdot \rho(z_j) = (c\rho)_j$ and $\Lambda(z_j) = \Lambda_j$, $\forall z_j \in \Omega_j$.

Assumption 3. Thermal conductivity tensor Λ_j can either be reduced to a scalar value λ_j for isotropic

conduction throughout a system component or is assumed to be a diagonal matrix with orthotropic properties $\Lambda_j = \text{diag}(\lambda_{j,z_1}, \dots, \lambda_{j,z_{n_{\text{dim}}}})$.

The initial condition $T(z, 0) = T_0(z)$, $z \in \Omega$ sets an inhomogenous temperature distribution T_0 throughout the domain. Furthermore, heat transfer between surface and surrounding fluid or gas also known as *Robin* boundary conditions ϕ_R have to be accounted for. This boundary condition is formulated as superimposed heat flux $\text{phi}_R = \phi_{\text{conv}} + \phi_{\text{rad}}$ caused by heat emission ϕ_{rad} and convection ϕ_{conv} with defined on $z_B \in \partial\Omega$ as:

$$\phi_{\text{conv}}(z_B, t) = \alpha(T(z_B, t), z_B) (T(z_B, t) - T_{\text{amb}}), \quad (2)$$

$$\phi_{\text{rad}}(z_B, t) = \varepsilon(z_B) \sigma (T(z_B, t)^4 - T_{\text{amb}}^4). \quad (3)$$

Herein, z_B corresponds to coordinates of domain surface $\partial\Omega$ exposed to ambient. Convective heat flux ϕ_{conv} is calculated from temperature difference between surface and ambient temperature T_{amb} , multiplied with temperature and geometric dependent film coefficient $\alpha(T(z_B, t), z_B)$. Radiative heat flux ϕ_{rad} is nonlinear in temperature and can be computed by *Stefan-Boltzmann-law* with emission coefficient $\varepsilon(z_B)$ and *Stefan-Boltzmann* constant σ . Thus, a nonlinear partial differential equation:

$$\frac{\partial}{\partial t} T(z, t) = f(T(z, t), T_{\text{amb}}) \quad (4)$$

needs to be solved for $T(z, t)$. However, nonlinear equation (4) can be transformed into a linear parameter-variant (LPV) system description, if nonlinear dependencies are moved into system coefficients (Bruzelius, 2004). This is applicable for thermal systems. Thus, *Robin* boundary conditions are set to

$$\phi_R(z_B, T) = \alpha_{\text{tot}}(T(z_B), z_B) (T(z_B) - T_{\text{amb}}), \quad (5)$$

with total film coefficient:

$$\alpha_{\text{tot}}(T(z_B, t), z_B) = \alpha(T(z_B, t), z_B) + \frac{\phi_{\text{rad}}(z_B, t)}{T(z_B, t) - T_{\text{amb}}}. \quad (6)$$

Nevertheless, $\alpha_{\text{tot}}(T(z_B, t), z_B)$ still depends on local geometry and hence, is a function of z_B . However, it can be assumed as a surface area specific function:

Assumption 4. *Superimposed film coefficient function $\alpha_{\text{tot}}(T(z_B, t), z_B)$ is spatially independent throughout specific surface areas $\partial\Omega_i \subset \partial\Omega$, $i \in \{1, \dots, n_{\text{surf}}\} \subset \mathbb{N}^+$, leading to discrete $\alpha_{\text{tot}}(T(z_{B,i}, t), z_{B,i}) = \alpha_{\text{tot},i}(T(z_{B,i}, t))$, $\forall z_{B,i} \in \partial\Omega_i$.*

According to (Frank et al., 2019) area-specific film-coefficient functions are approximated by shape-preserving piece-wise cubic interpolation at predefined query points. Thus, identifiable parameters

p_α are created to parametrize temperature dependent boundary conditions. Moreover, $p_{cp} \in \mathbb{R}^{n_{\text{comp}}}$ and $p_\lambda \in \mathbb{R}^{n_{\text{comp}} \cdot n_{\text{dim}}}$ describe material properties. Combined parameter vector $p \in \mathcal{P} \subseteq \mathbb{R}^{n_p}$ contains all of the variant system parameters. Domain Ω is spatially discretized using weak formulation and finite element method to get a lumped element model. This results in a system of linear-parameter variant ordinary differential equations (ODEs) (Huang and Usmani, 1994), (Li and Qi, 2010). First order shape functions $f_s^T(z) : x(t) \mapsto T(z, t)$ are used to map node temperatures $x \in \mathbb{R}^{n_x}$ of finite element mesh to continuous temperature distribution $T(z, t)$. Eventually, following system description is obtained and can be exported from finite element analysis, but only at a specific operating point with constant parameters \hat{p} ,

$$E|_{\hat{p}_{cp}} \dot{x} = A|_{\hat{p}_\alpha, \hat{p}_\lambda} x + B|_{\hat{p}_\alpha} u, \quad (7)$$

with damping matrix $E \in \mathbb{R}^{n_x \times n_x}$, conductivity matrix $A \in \mathbb{R}^{n_x \times n_x}$, load matrix $B \in \mathbb{R}^{n_x \times n_u}$, and input vector $u \in \mathbb{R}^{n_u}$. All of the matrices are in numeric form, but accessible parameters are required. Thus, a form of affine parameter dependence is formulated for the matrices similar to (Feng et al., 2016). In regard to assumptions 1 and 2, matrices are specified as:

$$E(p_{cp}) \approx E_0 + \sum_{j=1}^{n_{\text{comp}}} E_{cp,j} \cdot p_{cp,j}, \quad (8)$$

$$A(p_\alpha, p_\lambda, x) \approx A_0 + A_\alpha \odot P_{A,\alpha}(x) + \sum_{j=1}^{n_{\text{comp}}} \sum_{k=1}^{n_{\text{dim}}} A_{\lambda,k,j} \cdot p_{\lambda,k,j}, \quad (9)$$

$$B(p_\alpha) \approx B_0 + B_\alpha \odot P_{B,\alpha}(x). \quad (10)$$

Component-specific matrices $E_{cp,j}$ and $A_{\lambda,k,j}$ are multiplied with the corresponding material properties. In the equations above n_{comp} describes the components with varying parameters. Parameter that are already known or of less significance can be considered by E_0 and A_0 . These matrices are extracted from linearized numerical matrices by setting the varying parameters near zero. $E_{cp,j}$ and $A_{\lambda,k,j}$ are formulated according to the following component-wise (j) matrix export

$$E_0 = E|_{(\hat{p}_{cp} \rightarrow 0)}, \quad (11)$$

$$E_{cp,j} = E|_{(\hat{p}_{cp,j}=1)} - E_0, \quad (12)$$

$$A_0 = A|_{(\hat{p}_\lambda \rightarrow 0, \hat{p}_\alpha \rightarrow 0)}, \quad (13)$$

$$A_{\lambda,k,j} = A|_{(\hat{p}_{\lambda,k,j}=1, \hat{p}_\alpha \rightarrow 0)} - A_0, \quad (14)$$

$$B_0 = B|_{(\hat{p}_\alpha \rightarrow 0)}, \quad (15)$$

$$A_\alpha = \sum_{i=1}^{n_{\text{surf}}} A|_{(\hat{p}_\lambda \rightarrow 0, \hat{p}_{\alpha,i}=1)} - A_0, \quad (16)$$

$$B_\alpha = \sum_{i=1}^{n_{\text{surf}}} B|_{(\hat{p}_{\alpha,i}=1)} - B_0. \quad (17)$$

Matrices $P_{A,\alpha}(x) \in \mathbb{R}^{n_x \times n_x}$ and $P_{B,\alpha}(x) \in \mathbb{R}^{n_x \times n_u}$ are multiplied to corresponding differential matrices with element-wise *Hadamard* product \odot and contain state(node)-specific film-coefficients. Every matrix entry represents a node, that is assigned to a component or surface. Thus, parameters p_α , including spline approximation parameters, can be used to construct $P_{A,\alpha}(x)$ and $P_{B,\alpha}(x)$. These matrices are state dependent, because thermal boundary conditions vary with temperature. Eventually, a LPV description derived from numerical FEA is generated including physically interpretable parameters

$$E(p_{cp})\dot{x} = A(p_\alpha, p_\lambda, x)x + B(p_\alpha, x)u. \quad (18)$$

2.2 Model Order Reduction

System descriptions derived from FEA tend to have large scale, especially if complex geometries or multiple components are present. Thus, computation-costs are very high and prevent real-time capable execution or high amount of simulation iterations for optimization problems. If model simplifications, symmetry or reduction in spatial dimensions are infeasible, model order reduction methods can be powerful tools, to further reduce computation time with sufficiently accurate simulation results. However, most approaches are only valid for linear system descriptions. Moreover, physical interpretation of reduced systems and parameter access is no longer possible, since the reduced states do not represent temperatures. Hence, already validated full order models are required and have to be linearized at an operating point. Parametric model order reduction methods are used as a remedy, but are limited to constant parameters or further extend reduced system descriptions. Data-based methods are based on system snapshots, which can be difficult to obtain, if no measurement data can be acquired or multiple time-consuming simulations of a full order model have to be performed. A promising remedy has been introduced in (Frank et al., 2018), where system description (18) is split into a linearized part and an additive function to correct operating point deviations. Classical model order reduction for linear systems is used to calculate projectors, that are also applied to the corrective function. A similar approach is used in this work, as model order reduction is calculated for a linearized system and parameter variation are added subsequently. Thus, time consuming reduction algorithms are performed only once, and parameter variations or state dependent changes can be accounted for separately. For applying projection-based model reduction, an arbitrary operating point \hat{p} can be inserted in equation

(18) to obtain a linear system (7), without repeated export of numerical matrices from FEA. Model order reduction using Rational Krylov projections (Grimme, 1997) has been found to be most robust in approximating system behaviour with subsequent deviations from chosen operating point. In this method moments of the original transfer function are approximated at predefined frequency shifts, so that as many moments as possible are matched between original and reduced order system. Eventually, linear projectors $W \in \mathbb{R}^{n_x \times q}$ and $V \in \mathbb{R}^{n_x \times q}$ are obtained from applied model order reduction with reduced dimension $q \ll n$. Hence, reduced matrices $\tilde{A}|_{\hat{p}_\alpha, \hat{p}_\lambda} = W^T A|_{\hat{p}_\alpha, \hat{p}_\lambda} V$, $\tilde{A}|_{\hat{p}_\alpha, \hat{p}_\lambda} \in \mathbb{R}^{q \times q}$, $\tilde{B}|_{\hat{p}_\alpha} = W^T B|_{\hat{p}_\alpha}$, $\tilde{B}|_{\hat{p}_\alpha} \in \mathbb{R}^{q \times n_u}$, $\tilde{E}|_{\hat{p}_{cp}} = W^T E|_{\hat{p}_{cp}} V$, $E|_{\hat{p}_{cp}} \in \mathbb{R}^{q \times q}$, and projected state vector $\tilde{x} \in \mathbb{R}^q$ can be calculated. Transformation between state-vectors can be expressed as:

$$\tilde{x} = W^T x, \quad x \approx \bar{x} = V \tilde{x}, \quad (19)$$

with approximated full order state vector $\bar{x} \in \mathbb{R}^{n_x}$. Reduced system description at operating point \hat{p}

$$\tilde{E}|_{\hat{p}_{cp}} \dot{\tilde{x}} = \tilde{A}|_{\hat{p}_\alpha, \hat{p}_\lambda} \tilde{x} + \tilde{B}|_{\hat{p}_\alpha} u \quad (20)$$

is extended to consider material uncertainties, using affine characteristics of equations (8) and (9). Thus, damping and system matrix are obtained from:

$$\tilde{E} = \tilde{E}|_{\hat{p}_{cp}} + W^T \left[\sum_{j=1}^{n_{comp}} E_{cp,j} \cdot (p_{cp,j} - \hat{p}_{cp,j}) \right] V, \quad (21)$$

$$\tilde{A} = \tilde{A}|_{\hat{p}_\alpha, \hat{p}_\lambda} + W^T \left[\sum_{j=1}^{n_{comp}} \sum_{k=1}^{n_{dim}} A_{\lambda,k,j} \cdot (p_{\lambda,k,j} - \hat{p}_{\lambda,k,j}) \right] V, \quad (22)$$

$$\tilde{B} = \tilde{B}|_{\hat{p}_\alpha}. \quad (23)$$

Since, projectors are applied although approximated transfer function of the original system varies, applicability of introduced transformations has to be investigated. It is obvious that amount of material properties and deviation is limiting overall approximation quality. For thermal systems with rather sluggish system dynamic, a variation of damping parameters is not as crucial as a variation of thermal conductivity, especially if transfer function moments at lower frequency shifts are approximated. Detailed results are presented in section 3. For identification purposes or process planning, these changes can be made before the simulation is started. However, state dependent change of boundary conditions have to be accounted for during the computation. Thus, *online* correction of film-coefficients introduced in (Frank et al., 2018) is used. Therefore, additionally to previous equations, a non-constant state-dependent term g is added to system matrix \tilde{A}

and input matrix \tilde{B} . In order to reduce computation-effort, g is not updated in every simulation time step. Instead, it is kept piece-wise constant unless surface temperatures $x_\alpha \in \mathbb{R}^{n_\alpha}$ change more than a pre-defined threshold T_{thres} . Thus, a balancing option between computation time and simulation accuracy is created and piece-wise constant corrector function $g_*(p_\alpha, x_\alpha^*, T_{\text{amb}}^*) : \mathbb{R}^{n_p} \times \mathbb{R}^{n_\alpha} \times \mathbb{R} \rightarrow \mathbb{R}^q$ is formulated as:

$$g_* = H \cdot [C_\alpha A_\alpha C_\alpha^T \odot f_\alpha(p_\alpha^* - \hat{p}_\alpha, x_\alpha^*) x_\alpha^* + C_\alpha B_\alpha \odot f_{\alpha,B}(p_\alpha^* - \hat{p}_\alpha, x_\alpha^*) T_{\text{amb}}^*] \quad (24)$$

with *offline* calculable matrices $C_\alpha A_\alpha C_\alpha^T$, $C_\alpha B_\alpha$, and $H = W^T C_\alpha^T$, $H \in \mathbb{R}^{q \times n_\alpha}$. The surface states affected by temperature-dependent boundary conditions, can be extracted with binary matrix $C_\alpha \in \mathbb{R}^{n_\alpha \times n_x}$ $x_\alpha = C_\alpha x$. Functions $f_\alpha : \mathbb{R}^{n_\alpha} \times \mathbb{R}^{n_\alpha} \rightarrow \mathbb{R}^{n_\alpha} \times \mathbb{R}^{n_\alpha}$ and $f_{\alpha,B} : \mathbb{R}^{n_\alpha} \times \mathbb{R}^{n_\alpha} \rightarrow \mathbb{R}^{n_\alpha} \times \mathbb{R}^{n_u}$ expresses surface-node specific film-coefficient deviations from spline parameters and query temperatures x_α^* . Thus, computation-efficient state space formulation

$$\tilde{E} \dot{\tilde{x}}(t) = \tilde{A} \tilde{x}(t) + \tilde{B} u(t) + g_*(p_\alpha, x_\alpha^*, T_{\text{amb}}^*) \quad (25)$$

is obtained and discretized in time using implicit euler method. Thus, larger time-steps can be chosen without affecting simulation stability. Output equation for temperatures at points of interest $T_S \in \mathbb{R}^{n_s}$ is formulated by selecting node temperatures with a binary matrix $C \in \mathbb{R}^{n_s \times n_x}$. With applied order reduction projectors, output equation is formulated as $T_S = \tilde{C} \tilde{x}$.

3 RESULTS

In this section, two exemplary thermal systems are introduced to validate the proposed modeling approach. Subsequently, parameter variation studies are presented for different materials. A parameter identification and validation results are mentioned in the final subsection.

3.1 Exemplary Thermal Systems

A plane rubber specimen and a heating plate are used to exemplify the modeling approach from the previous section and to verify parameter identification with measurement data. The rubber specimen consists of a rubber compound with two temperature sensors placed near the center-line of the cross-section (see Figure 1a). Its dimensions are $25 \text{ cm} \times 20 \text{ cm} \times 2 \text{ cm}$. The full order model is created in a 2D-plane with $n_{x,\text{rub}} = 5271$ nodes, representing the central cross-section. The reduction is performed with moment

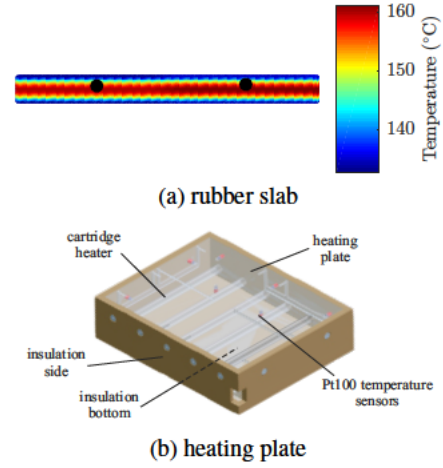


Figure 1: Exemplary thermal systems plane rubber specimen (a) and heating plate (b).

matching and empirically determined shifts, leading to reduced dimension $q_{\text{rub}} = 21$. In addition an adequate heating plate is used for curing processes (Figure 1b) (Bosselmann et al., 2017). The heating plate is made of aluminum alloy. A 10mm thick layer out of thermoplastic resin polyetheretherketon (PEEK) is added to side and bottom surface for insulating purposes. Six electric cartridge heater and $n_s = 12$ Pt100 sensors are embedded into the heating plate. The sensors are placed 5mm underneath the aluminum surface and are used to approximate surface temperature distribution. Each cartridge heater has a maximum power of 825W and is divided into three segments each, resulting in 18 independently controllable segments with a maximum power of 275W. Due to a slightly asymmetrical build and volumetric heat generation, the model is created in 3 dimensions. Dimension $n_{x,\text{HP}} = 29173$ is reduced to $q_{\text{HP}} = 95$.

3.2 Parameter Variation

This section presents the results of modeling parameter variations. These variations can be taken into account by using Equations (21) and (22). According to the presented method, projectors of model order reductions are calculated at a predefined parameter vector \hat{p} . This reduced order model is used to approximate original system states \bar{x}_0 at \hat{p}_0 and is kept as ground truth, since the projectors are specifically calculated for this scenario. Subsequently, multiple reduced order models are constructed at different parameter vectors \hat{p}_m . These models are then corrected to match the system at \hat{p}_0 according to Equations (21) and (22). Since the projectors are calculated for the ground truth at \hat{p}_0 , approximation errors occur. For the rubber sample system it is assumed that material

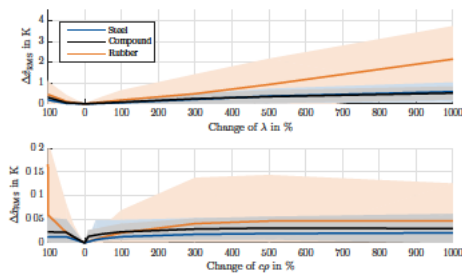


Figure 2: Rubber specimen material parameters verification results for a sample curing process. Tolerance bands depict highest deviation for a single state.

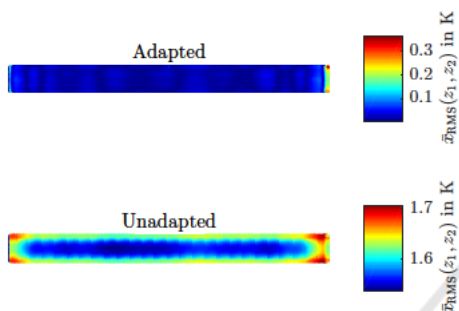


Figure 3: Distribution of state deviation with $\bar{x}_{RMS}(z_1, z_2)$ calculated over all time-steps for a material parameter deviation of 10% in the rubber specimen. With no parameter adaption such small deviations can lead to a significant temperature error (lower picture), whereas the proposed method shows accurate results throughout the whole cross-section.

properties λ and c_p are varying. Deviation between corrected systems and original reduced system at \hat{p}_0 is depicted in Figure 2.

The error $\Delta \bar{x}_{RMS}$ is calculated for all simulated time-steps K and for all reconstructed states $\bar{x} \in \mathbb{R}^{n_x}$ of the rubber cross-section. Moreover, tolerance bands are shown to represent minimal and maximal error for the worst approximated states in the cross-section. Three different materials are chosen to represent low (rubber), medium (compound) and high (steel) thermal conductivity and different specific heats/densities, respectively. Especially for small parameter deviations around the operating point, used to calculate reduction projectors V, W , a correction without costly recalculation of the reduction is a valid approach.

Spatial distribution of temperature errors are depicted in Figure 3, if material parameters (λ and c_p) of the rubber specimen vary with 10%. The lower illustration shows the deviation $\bar{x}_{RMS}(z_1, z_2)$ calculated over all simulated timesteps, if no further adaption is made to the model. The upper figure depicts a proper adaption in regard to the proposed method. It can be stated that throughout the whole cross-section a precise approximation of temperature can be achieved.

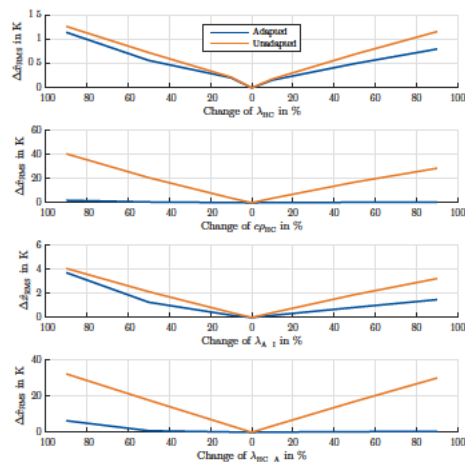


Figure 4: Adaption results of material and heat transition parameters for the heating plate model. Blue indicates results for adapted parameters according to the proposed method, whereas orange depicts model errors with no adaptations.

Similar results arise for material properties and heat transitions parameters of the heating plate model. Figure 4 depicts parameter adaption results for the heating plate. 4 parameters are assumed to be unknown or varying. Material parameters of the heating cartridges $c_{p_{HC}}, \lambda_{HC}$ as well as heat transitions between aluminum and heating cartridges λ_{HC-A} , insulation material λ_{A-I} . Deviation for all states is shown if no adaption of parameter variation is considered (orange) and parameters are adapted according to the proposed method (blue). It can be stated that accuracy is significantly increased, if parameter adaption is considered. Moreover the same conclusion as for the rubber specimen can be made: For slight changes around the initial operating point, the proposed method is applicable to accurately approximate system behaviour. Thus, it is well suitable to identify unknown parameters, with sufficiently accurate results if the initial guess is not completely unadequate. Identification procedures and results are presented in the subsequent section.

3.3 Parameter Identification and Verification

Since rubber is a natural product, thermal material properties ($p_{rub, cp}, p_{rub, \lambda}$) of the compound may vary. Moreover, due to previous processes geometric variation such as a thickness can alter. With the use of orthotropic material properties, thermal conductivity in this direction $p_{rub, \lambda_{thick}}$ can be adapted separately. Moreover, during cooling processes at ambient temperature, temperature depen-

dent film-coefficient functions need to be identified and frequently adapted. Two functions are used for top and bottom each, approximated with splines at 3 query temperatures, leading to $p_{\text{rub},\alpha} \in \mathbb{R}^6$. Thus, overall $p_{\text{rub}} \in \mathbb{R}^9$ parameters need to be identified for the plane rubber specimen $p_{\text{rub}} = (p_{\text{rub},c,p}, p_{\text{rub},\lambda}, p_{\text{rub},\lambda_{\text{thick}}}, p_{\text{rub},\alpha})^T$.

Unknown parameters for the heating plate are heat transitions between heating cartridges and aluminum ($p_{\text{HC-A},\lambda}$) as well as between aluminum and insulation ($p_{\text{A-I},\lambda,4}$). Furthermore, material properties of heating cartridges ($p_{\text{HC},c,p}, p_{\text{HC},\lambda}$) and film-coefficient functions for bottom and side insulation and metal surfaces are unknown ($p_{\text{HP},\alpha}$). Since three different surfaces are approximated with 3 query points each, 9 film coefficient parameters have to be identified. This results in 12 identifiable parameters p_{HP} for the heating plate. In order to determine the parameters of both systems, an optimization problem is formulated to minimize the temperature deviation between measurement T_{meas} and simulation output T_S at the given sensor positions. For all simulated time-steps K cost-function J is calculated as

$$\min_p J(p) = \sqrt{\frac{1}{n_S} \sum_{s=1}^{n_S} \frac{1}{K} \sum_{k=1}^K [T_{S,k,s}(p) - T_{\text{meas},k,s}]^2}. \quad (26)$$

It is obvious that for a large dimension of the affiliated parameter vector p , computation-effort and complexity of the optimization problem increases. For large system scale all solving algorithms based on multiple iterations are not a feasible approach. Hence, the proposed modeling method is a promising remedy to arising conflicting goals between number of parameters, simulation accuracy and computation time, since it allows for more options to balance between them. Thus, *Particle Swarm Optimization* (PSO) with a vast amount of required simulation iterations is used to find the global minimum of cost function J and identify unknown parameters. For the heating plate update threshold $T_{\text{thres,HP}}$ of thermal boundary conditions is set to 1 K and a time step of 5 s is used. This results in a computation time of approximately 0.3 s, if a 60 min curing process is simulated. Thus, whole optimization duration is about half an hour for 6000 iterations on a Dual-Core Intel Core i5-4690 3.5 GHz. Residual cost function value is $J_{\text{min,HP}} = 0.7$ K. Verification results for a sample heating process are depicted in Figure 5. Overall conformity between measured and simulated temperature at sensor positions is sufficiently accurate, whereas load changes lead to higher short term deviations. Main cause are different heat transitions for each heating cartridge and thermal dependencies of material properties have been neglected, only film-coefficients are frequently corrected.

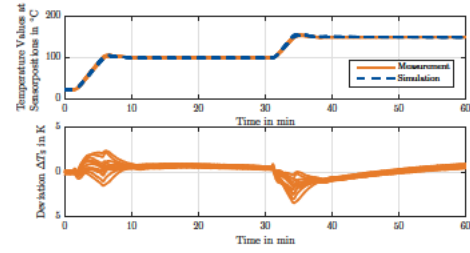


Figure 5: Heating plate parameters verification results for a sample heating process.

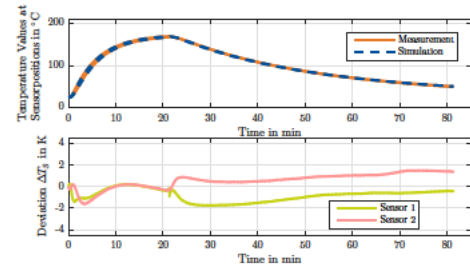


Figure 6: Rubber specimen parameters verification results for a sample curing process.

During a curing process, the rubber specimen is heated up and subsequently cooled down. Thus, a model for heating inside the mold and a model for cool down at ambient temperature is required. The inhomogeneous initial conditions of the cooling phase can be accounted for, by splitting the system into load dynamic and initial condition response (Beattie et al., 2017) and perform model order reduction separately for both dynamics. Figure 6 depicts parameter validation results for a sample curing process. The heating process finishes at 22 min. Until then no temperature dependent boundary conditions occur since the rubber is enclosed in the mold and thus, no triggered additive function g is required. For the cooling process strong nonlinear temperature dependencies have to be accounted for, by using the triggered function g to correct the deviation to the operating point. Overall accuracy at sensor positions is well inside a 2 K tolerance, which is sufficiently accurate for this process example.

4 CONCLUSION

A method for reduced-order thermal modeling of parameter variations for parameter identification in process planning and control is presented in this manuscript. Therefore, a generic approach is described to extract parameter dependencies from numerical models. The heat equation with temperature dependent boundary conditions is used to calcu-

late temperature distributions over time in 2 or 3 dimensional problems. Since large system scales can arise from finite element analysis, model order reduction is applied to reduce computation time. This computation-efficient description is required for solving optimization problems with a high amount of iterations or meeting real-time demands. However, basic model order reduction methods are only valid for linear models. If the system can not be linearized properly, temperature dependent boundary conditions as well as parameter uncertainties have to be accounted for. Parametric reduction algorithms are either based on system snapshots or entail higher reduced orders and larger projection matrices. Thus, a method to preserve physically interpretable parameters, while using rational Krylov model order reduction algorithms is proposed. This is especially applicable for small variations around a well defined initial operating point. Hence, neither a validation of the full order model before formulating the reduced model is required nor many time consuming experiments to get measurement data. Instead system parameters are identified and validated with a reduced system formulation. Moreover, temperature dependencies during the process can be modeled and a parameterizable balancing between computation time and accuracy is possible. Thus, online process adaptations according to (stochastic) parameter variations are possible without costly recalculation of model order reduction. The approach is demonstrated for two sample systems, which material and heat transition parameters are identified with reduced-order models. Therefore, particle swarm optimization can be used to find the global minimum of a formulated cost-function. Moreover, computation times are within real-time restrictions and thus, presented models are used for model-based temperature control, process predictions and state estimation.

REFERENCES

- Aleksendrić, D., Carlone, P., and Čirović, V. (2016). Optimization of the temperature-time curve for the curing process of thermoset matrix composites. *Applied Composite Materials*, 23(5):1047–1063.
- Astrid, P. (2004). *Reduction of process simulation models : a proper orthogonal decomposition approach*. PhD thesis, Department of Electrical Engineering.
- Beattie, C., Gugercin, S., and Mehrmann, V. (2017). Model reduction for systems with inhomogeneous initial conditions. *Systems & Control Letters*, 99:99 – 106.
- Benner, P., Gugercin, S., and Willcox, K. (2015). A survey of projection-based model reduction methods for parametric dynamical systems. *SIAM Review*, 57(4):483–531.
- Benner, P., Herzog, R., Lang, N., Riedel, I., and Saak, J. (2019). Comparison of model order reduction methods for optimal sensor placement for thermo-elastic models. *Engineering Optimization*, 51(3):465–483.
- Bosselmann, S., Frank, T., Wielitzka, M., Dagen, M., and Ortmaier, T. (2017). Thermal modeling and decentralized control of mold temperature for a vulcanization test bench. In *2017 IEEE Conference on Control Technology and Applications (CCTA)*, pages 377–382.
- Bosselmann, S., Frank, T., Wielitzka, M., and Ortmaier, T. (2018). Optimization of process parameters for rubber curing in relation to vulcanization requirements and energy consumption. In *2018 IEEE/ASME International Conference on Advanced Intelligent Mechatronics (AIM)*, pages 804–809.
- Bruzelius, F. (2004). *Linear parameter-varying systems: An approach to gain scheduling: Zugl.: Goteborg, Univ., Diss., 2004*. PhD thesis, School of Electrical Engineering.
- Chaturantabut, S. and Sorensen, D. C. (2010). Nonlinear model reduction via discrete empirical interpolation. *SIAM Journal on Scientific Computing*, 32(5):2737–2764.
- Feng, L., Yue, Y., Banagaaya, N., Meuris, P., Schoenmaker, W., and Benner, P. (2016). Parametric modeling and model order reduction for (electro-)thermal analysis of nanoelectronic structures. *Journal of Mathematics in Industry*, 6(1):10.
- Frank, T., Bosselmann, S., Wielitzka, M., and Ortmaier, T. (2018). Computation-efficient simulation of nonlinear thermal boundary conditions for large-scale models. *IEEE Control Systems Letters*, 2(3):351–356.
- Frank, T., Wieting, S., Wielitzka, M., Bosselmann, S., and Ortmaier, T. (2019). Identification of temperature-dependent boundary conditions using mor. *International Journal of Numerical Methods for Heat & Fluid Flow*, ahead-of-print.
- Grimme, E. (1997). *Krylov Projection Methods for Model Reduction*. PhD thesis, Department of Electrical and Computer Engineering.
- Huang, H.-C. and Usmani, A. S. (1994). *Finite Element Analysis for Heat Transfer*. Springer London, London.
- Li, H.-X. and Qi, C. (2010). Modeling of distributed parameter systems for applications - a synthesized review from time & space separation. *Journal of Process Control*, 20(8):891 – 901.
- Speicher, K., Steinboeck, A., Kugi, A., Wild, D., and Kiefer, T. (2014). Analysis and design of an extended kalman filter for the plate temperature in heavy plate rolling. *Journal of Process Control*, 24(9):1371 – 1381.
- Sun, C. and Hahn, J. (2006). Model reduction in the presence of uncertainty in model parameters. *Journal of Process Control*, 16(6):645 – 649.
- Wang, D.-h., Dong, Q., and Jia, Y.-x. (2015). Mathematical modelling and numerical simulation of the non-isothermal in-mold vulcanization of natural rubber. *Chinese Journal of Polymer Science*, 33(3):395–403.
- Yuan, C. D., Rudnyi, E. B., Baumgartl, H., and Bechtold, T. (2017). Model order reduction and system simulation of a machine tool for real-time compensation of thermally induced deformations. In *2017 IEEE International Conference on Advanced Intelligent Mechatronics (AIM)*, pages 1071–1076.